PROCEEDINGS OF THE ROYAL SOCIETY A MATHEMATICAL, PHYSICAL & ENGINEERING SCIENCES

Paradigm shifts in surface metrology. Part II. The current shift

X Jiang, P.J Scott, D.J Whitehouse and L Blunt

Proc. R. Soc. A 2007 **463**, 2071-2099
doi: 10.1098/rspa.2007.1873

PROCEEDINGS OF THE ROYAL SOCIETY A

Proc. R. Soc. A (2007) **463**, 2071–2099
doi:10.1098/rspa.2007.1873
Published online 5 July 2007

Review

Paradigm shifts in surface metrology. Part II. The current shift

By X. Jiang[1,*], P. J. Scott[1,3], D. J. Whitehouse[1,2,3] and L. Blunt[1]

[1]*Centre for Precision Technologies, School of Computing and Engineering, University of Huddersfield, Queensgate, Huddersfield HD1 3DH, UK*
[2]*School of Engineering, University of Warwick, Gibbet Hill Road, Coventry CV4 7AL, UK*
[3]*Taylor Hobson, PO Box 36, 2 New Star Road, Leicester LE4 9JQ, UK*

This is the second part of the paper 'Paradigm shifts in surface metrology'. In part I, the three historical paradigm shifts in surface metrology were brought together, and the subsequent evolution resulting from the shifts discussed. The historical philosophy highlighted the fact that the paradigm shifts must be robust and flexible, meaning that surface metrology must allow for full control of surface manufacture and provide an understanding of the surface functional performance. Part II presents the current paradigm shift as a 'stepping stone', building on the above historical context. Aspects of surface geometry will also have to cater for surfaces derived from disruptive application, i.e. structured and freeform surfaces are identified candidates. The current shift is presented in three aspects: from profile to areal characterization; from stochastic to structured surfaces; and from simple geometries to complex freeform geometries, all spanning the millimetre to sub-nanometre scales. In this paradigm shift, the scale of surface texture is beginning to approach some of the geometrical features in micro/nano electro-mechanical systems devices and is becoming one of the most important functionality indicators. Part II will contextualize the current shifts in the discipline of surface metrology, and cement surface metrology in place in the ultra precision and nanotechnology age.

Keywords: surface texture; measurement; instrumentation; filtration; characterization; standardization

1. Introduction

There are two reasons for the current paradigm shift in the discipline of surface metrology.

(i) *The dawn of the nanotechnology age* (Royal Society Report 2004) has brought into clear focus the issues of our ability to measure and qualify commercial micro- and nanometre scale manufactured components. As the dimensions of a product become smaller, the importance of the surface and its properties become the dominant factor in the successful functionality of

* Author for correspondence (x.jiang@hud.ac.uk).

Received 17 December 2006
Accepted 24 May 2007

that product. Surface chemistry, tribology, stress state and geometry all combine to define the fitness for purpose of the product. Measurement of surface texture is becoming increasingly critical because of its direct link to part functionality. Manufactured items such as micro- and nanometre scale transistors, micro electro mechanical systems (MEMS) and nano electro mechanical systems (NEMS), optics and structured surface products are clear evidence of products where the surface plays the dominant role.

(ii) *The next generation of ultra-precision surfaces* (Research Council 2004) will not only be incredibly smooth, but also have the specification of surface form at levels approaching atomic magnitude. Such surfaces will relate to a wide range of devices and components, including microelectronics devices, where semiconductor surfaces have to be extremely flat in order to pack more and more transistors and other microscopic components into the same area, optics in ground- and space-based telescopes, in defence- and satellite-based imaging systems and in large laser facilities, where smooth surfaces with complex optical shapes are required with precision up to one part in 10^8. Similar accuracy is also required in implantable medical devices such as hip and knee joints, where micrometre form and nanometre roughness requirements are specified in order to reduce the generation of wear debris.

The desire to measure and quantify geometric products at all levels, including micrometre, nanometre and atomic will continue to lead surface metrology from: profile to areal characterization; stochastic to structured surfaces; and simple shapes to complex freeform geometries.

2. Current shift: profile to areal characterization

(*a*) *Classification of areal instruments*

Probably the first step in areal surface texture analysis is that taken by Williamson (1967–1968), who built the first micrometre surface topography measurement system in 1968, and Grieve *et al.* (1970), who built a system based on a Talysurf III in 1970. Both systems were essentially based on making measurement along parallel traces using conventional stylus systems. However, the progress in surface texture measurement was slow until the advent of the new generation of personal computers in the 1980s, making areal measurements more practical in terms of handling the large amount of data involved (Teague *et al.* 1982; De Chiffre & Nielsen 1987).

Commercial areal surface instruments gradually became available in the early 1990s. Somicronic in France and Taylor Hobson in the UK both developed contacting stylus systems, while in the USA WYKO developed a system based on optical interferometry. These early pioneering commercial systems allowed good surface visualization with a small number of statistical parameters to quantify the surface topography.

Today instrumentation techniques have matured, the instrumentation now adopting a wide range of principles include contacting stylus, phase-shifting interferometry, white-light interferometry, confocal microscopy, chromatic probe microscopy, structured light techniques, scanning electron microscopy, scanning tunnelling microscopy and atomic force microscopy.

Comparison of the capabilities of surface texture instrumentation can be achieved by using plots in the amplitude–wavelength plane (figure 1), as suggested by Stedman (Stedman 1987; Thomas 1998). Such a plot gives the working capabilities of an instrument in that plane with respect to instrument attributes such as resolution and range in the lateral and vertical dimensions, probe geometry, numerical aperture, scanning mechanisms and other instrument constraints. Vorburger *et al.* (1998) developed the basic scheme further. Now, such plots provide an invaluable guide to specifying metrology instrumentation for particular measurement needs.

(*b*) *Historical background for areal surface texture*

Although simple statistical descriptions such as peak-to-pit heights and surface slope (figure 2) were used at the beginning of areal surface texture characterization, the research first published concentrated on the difficult problem of specifying and characterizing areal features. In the 1970s, Nayak (1971) and Sayles & Thomas (1977) initially used five nearest-neighbour ordinates in areal surface data to define a peak or a pit. In order to investigate contact phenomena of random surfaces, Whitehouse & Phillips (1982), Whitehouse (1994) also initially defined three areal parameters: summit density; summit height; and summit curvature. These definitions, however, depended on sampling density, and the results could be distorted by measurement noise.

The major shift and development of new concepts in areal characterization of engineering surfaces came in 1990 with the European Community supported BCR research programme (BCR 3374/1/0/170/90/2 1990). Within this project, Stout, Sullivan and Dong developed an integrated method for characterizing and measuring engineering surfaces in 'three dimensions', and generated the first definitions of the so-called 'Birmingham 14 parameters' (Stout *et al.* 1993). In 1997, the EC issued a call for a requirement for a standard for areal surface characterization. The results, derived from this EC-sponsored research, entitled 'SurfStand' (E.C. Contract 1998) has formed the basis for areal 'three-dimensional' surface roughness standards (Blunt & Jiang 2003). Consequently, in 2002, a working group in ISO/TC 213 was set up to develop areal surface texture standards, the future ISO/TS 25178 series.

(*c*) *New concept for areal surface texture*

Traditional profile parameters provide a simple approach to control the manufacturing process: they monitor changes in the surface texture and indicate changes in the manufacturing process such as machine tool vibration or tool wear. Once a manufacturing process has been established that produces workpieces that function well, it is assumed that all that is necessary to maintain acceptable production is to control the manufacturing process by monitoring changes in surface texture. Profile surface texture parameters were not capable of diagnosing product functional performance directly.

The areal method attempts to characterize the fundamental and functional topographical features of the surface, including assessment of texture shape and direction, estimation of feature attributes and differentiation between connected

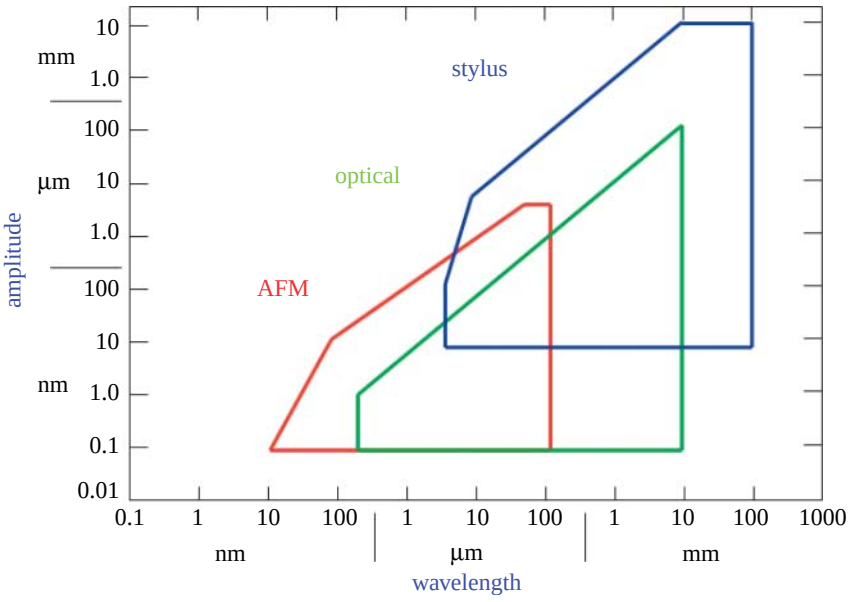

Figure 1. Example of typical amplitude–wavelength plots for AFM, optical and contact stylus instruments.

and isolated features. Areal surface characterization was not simply an extension from profile to the areal case (Stout *et al.* 1993; Blunt *et al.* 1999), but was a genuine attempt to characterize areal features.

(i) *Unified coordinate system for surface texture and form measurement*

Surface irregularities have traditionally been divided into three groups loosely based on lateral scale: (i) roughness (primary texture), generated by the material removal mechanism such as tool marks, (ii) waviness, produced by imperfect operation of a machine tool, and (iii) errors of form, generated by errors of a machine tool, distortions such as gravity effects, and also thermal effects, etc. This grouping gives the impression that surface texture should be part of a coherent scheme with roughness at the smaller scale, waviness at the intermediate scale and errors of form at the larger scale.

The primary definition of surface texture has, until recently, been based on the profile (ISO 4287: 1997). To ensure consistency of the irregularities in the measured profile, the direction of that profile was specified to be orthogonal to the lay (the direction of the predominant pattern of the surface irregularities). This direction is not necessarily related to the datum of the surface, whereas errors of form, such as straightness, are always specified as parallel to the datum of the surface (ISO 1101: 2004). Hence, profile surface texture and profile errors of form usually have different coordinate systems (figure 3) and, consequently do not form part of a coherent specification because they apply to different coordinate systems.

This situation has now altered since the draft standardization of areal surface methods, in which the primary definition of surface texture is changed from one being based on profiles to one based on areal surface. This means that there is no consistency requirement for the coordinate system to be related to the lay.

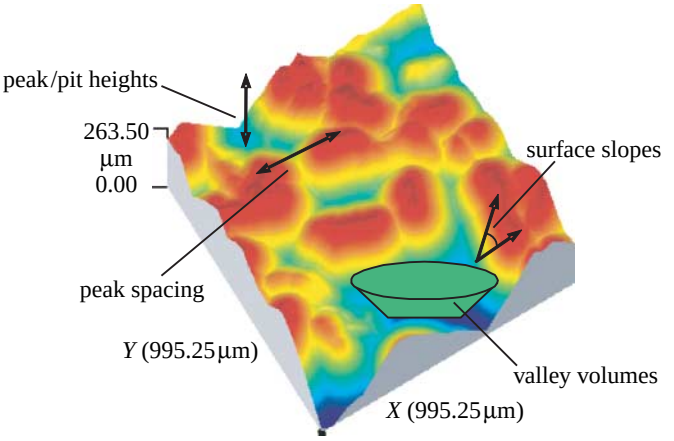

Figure 2. Some simple attributes used to characterize areal surface texture.

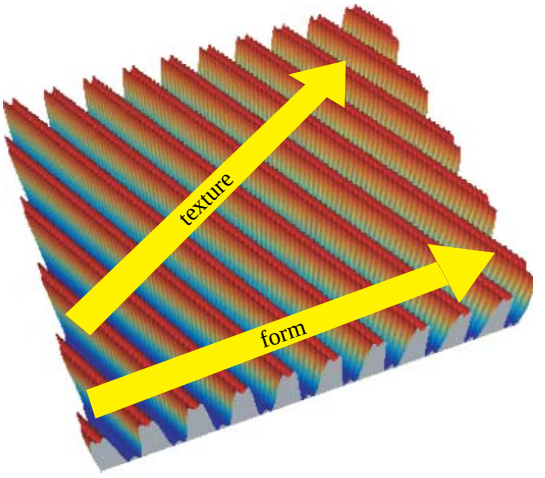

Figure 3. Profile texture and form had two different coordinate systems.

Therefore, a unified coordinate system has been established for both surface texture and form measurement (ISO/TS CD 25178-3: 2006). Surface texture is now truly part of a coherent scheme, with surface texture at the smaller scale, up to errors of form at a larger scale to part size at the largest scale (Jiang 2006). The system is known as the geometrical product specification (GPS).

(ii) *Scale-limited surface*

The other new concept for areal surface texture is the scale-limited surface. Different from the profile system, areal surface characterization does not require three different groups of surface texture parameters. For example, in areal parameters only Sq is defined for the root mean square parameter rather than the primary surface Pq, waviness Wq and roughness Rq in the profile case (ISO 4287: 1997). The meaning of the Sq parameter depends on the type of scale-limited surface used.

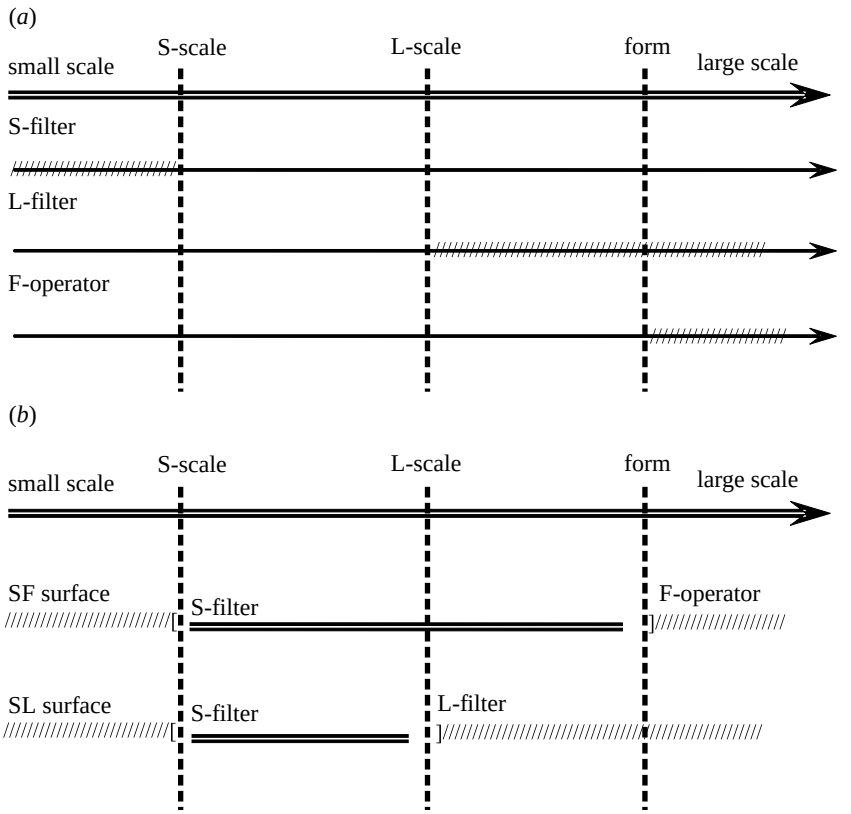

Figure 4. (*a*) Filters (S-filter or L-filter) and operator (F-operator), (*b*) and scale-limited surfaces (SF or SL surface) used in surface texture.

The S-filter removes unwanted small-scale lateral components of the surface such as measurement noise or functionally irrelevant small features. The L-filter removes unwanted large-scale lateral components of the surface and the F-operator removes the nominal form (figure 4*a*). The latter is called an operator rather than a filter (ISO/TS 17450-2: 2002) since it firstly uses optimization to determine a best fit to the nominal form, and then removes the fitted form from the surface.

An SF surface is obtained by using an S-filter and an F-operator in combination on a surface, and an SL surface by using an L-filter on an SF surface (figure 4*b*). Both SF and SL surfaces are called scale-limited surfaces.

The scale-limited surface depends on the filters or operators used, and is controlled by the nesting index (below) of those filters. The profile concept of a primary profile is equivalent in areal terms to the SF surface, with the nominal form removed by the F-operator and the profile λs filter equivalent to the areal S-filter. The profile concept of a roughness profile is equivalent in areal terms to the SL surface, with the profile λs filter equivalent to the areal S-filter and the profile λc filter equivalent to the areal L-filter. The profile concept of a waviness profile is equivalent in areal terms to the SF surface with the nominal form removed by the F-operator and the profile λc filter, equivalent to the areal S-filter.

A nesting index is an extension of the notion of the original cut-off wavelength and is suitable for all types of filters. For example, for a Gaussian filter, the nesting index is equivalent to the cut-off wavelength, and for a morphological filter with a spherical structuring element, the nesting index is the radius of the spherical element.

(*d*) *Numerical description*

An early numerical parameter set for areal surface texture was the 'Birmingham 14 parameters' (Stout *et al.* 1993; Dong *et al.* 1994*a*,*b*). This parameter set, though widely accepted, was considered to be somewhat of a 'theoretical nature' with insufficient practical evidence for its applicability (Lonardo *et al.* 1996; Peters *et al.* 2001). There were, however, still some problems with the definitions of the Birmingham 14 parameters: the mathematical descriptions in certain instances were ambiguous. For example, when the 'connectedness' of peaks or pits on a random surface is considered, how does one calculate the number of peaks or pits and their mean size as a function of height from the reference surface? How do peaks join together to form ridges, or how do pits link up? Furthermore, suitable parameters relevant to the material ratio curve need to be more indicative, in order to characterize common functional properties such as area and volume geometrical properties, or to describe wear and tribological properties.

Under the SurfStand Project (E.C. Contract 1998), the parameters for areal surface texture were further assessed with respect to stability, reliability and functional capabilities by a consortium formed by both academia and industry. Improvement and verification work was carried out with the emphasis on much stronger practical evidence and more feasible applications. The surface texture areal parameters derived from this research were developed according to their geometrical properties and partitioned into two main classes called 'field' and 'feature' parameters.

The field parameters are based on statistics, and are used to classify averages, deviations, extremes and specific features from a scale-limited continuous surface. The feature parameters are a new concept for surface texture and are defined using subsets of pre-defined features from a scale-limited continuous surface by using segmentation based on pattern recognition (Scott 2004). This concept allowed dominant topographical features to be identified and catalogued (for details see §3). The field and feature parameter sets (Blunt & Jiang 2003) form the core part of the new basis for an ISO technical specification for areal surface texture (ISO/TS CD 25178-2: 2006).

(*e*) *The field parameter set*

The field parameter set consists of the S-parameters and the V-parameters. The S-parameters depend on the height amplitude and spacing frequency, to describe both amplitude and spatial information. The V-parameters give fundamental volumetric information based on the areal material ratio curve (Abbott–Firestone curve).

The S-parameter set contains 12 parameters (ISO/TS CD 25178-2: 2006) and has been divided into four basic types: height; spacing; hybrid; and miscellaneous, as shown in figure 5. The height parameters depend on the

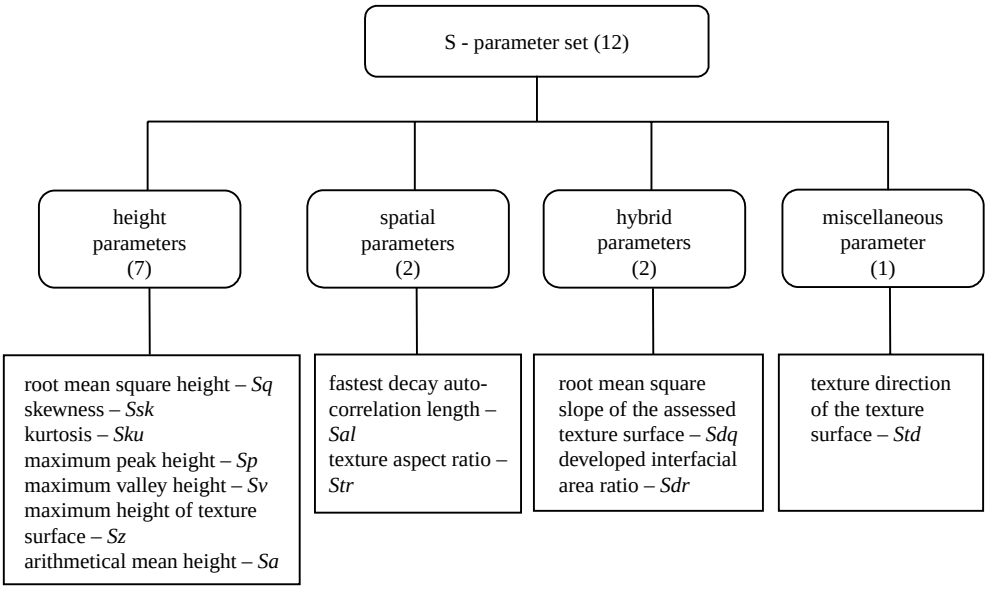

Figure 5. The S-parameter set.

amplitude deviation, to describe amplitude-related properties of a surface. They mirror the profile amplitude parameters since many industrial users wanted continuity with the profile amplitude parameters. The spacing parameters refer to the spatial properties of surfaces. *Sal* and *Str* parameters are designed to assess areal aspects of surface texture, including texture strength and uniformity of the texture in all directions, and they are particularly useful in distinguishing between highly textured and random surface structures, and monitoring machine tool vibration and chatter (Jiang & Blunt 2003). The hybrid parameters *Sdq* and *Sdr* are based on both amplitude and spatial information. They define numerically hybrid topography properties such as the slope of the surface and the interfacial area. Since most contact occurs on the flanks of peaks, and hybrid parameters contain information about peak flanks, hybrid parameters have particular relevance to the contact properties, both electrical and thermal, sealing properties, and wear and optical reflectance properties of a surface (Greenwood & Williamson 1966). There is one miscellaneous parameter *Std*, which is designed to provide information in the texture direction, such as the lay direction of the surface texture.

The V-parameter set (ISO/TS CD 25178-2: 2006) in figure 6 is designed to assess the functional topographical features of the surface through analysing the material volume and void volume of a scale-limited surface. The rationale behind the parameters is to split the material ratio curve of a surface into three height zones, the peak, the core and the valley zones, and then to make volume calculations based on the three zones. The splitting of the material ratio curve into three zones was originally derived from DIN 4476 (1990), as a practical solution to bearing problems in the automotive industry. The main idea is that the peak zone corresponds to initial running-in wear, the core zone to wear throughout the lifetime of the component, and the valley zone to lubricant retention under heavy wear conditions.

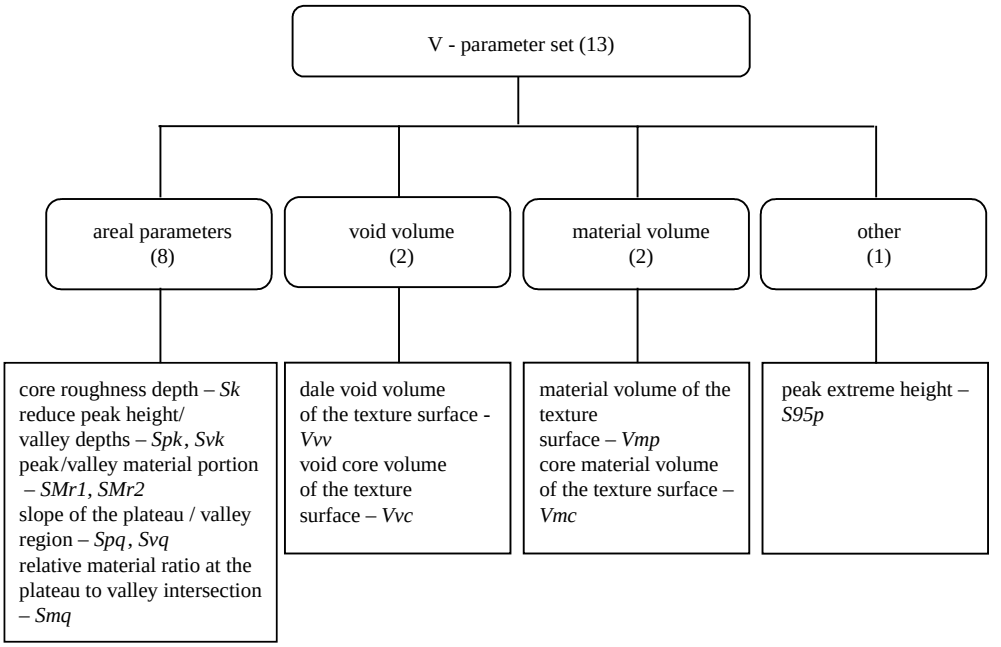

Figure 6. The V-parameter set.

(*f*) *Multi-scale analysis*

It is recognized that the manufacture of ultra-precision surfaces leaves multi-scale topography signatures within the topography of the surface. In practice, this means that a surface will contain fine-scale texture, from multiple sources, superimposed on other scales of texture. For example, the surface topography of a machined surface contains the information appertaining to the machine tool, including tool marks, machine vibrations and manufacturing conditions. The multi-scale nature of topography is an important factor in the functional performance of the surface. In bio-implant applications, for example, these variations will influence the wear properties of the surface and even biological interactions. These influences have long been recognized, and the traditional profile-based definitions of roughness, waviness and form are attempts to address them. The fundamental problem, however, has always been the efficient extraction, adequate reconstruction and preservation of the multi-scale information contained within the topography.

Wavelet theory provides a new analysis tool capable of resolving this fundamental problem; it employs space–frequency windows and offers the relevant space–frequency analysis. Wavelet transforms can divide functions into different scale–frequency components, and then each component can be studied with a resolution matched to its scale (Chui 1992; Daubechies 1992). Progress in wavelet analysis created an opportunity that enabled researchers such as Jiang & Li (1994) and Chen *et al.* (1995) to use orthogonal wavelets to decompose machined turned, milled and ground surfaces, and evaluate the tool marks, machining vibrations and machine-tool errors. An example of a milled surface is shown in figure 7.

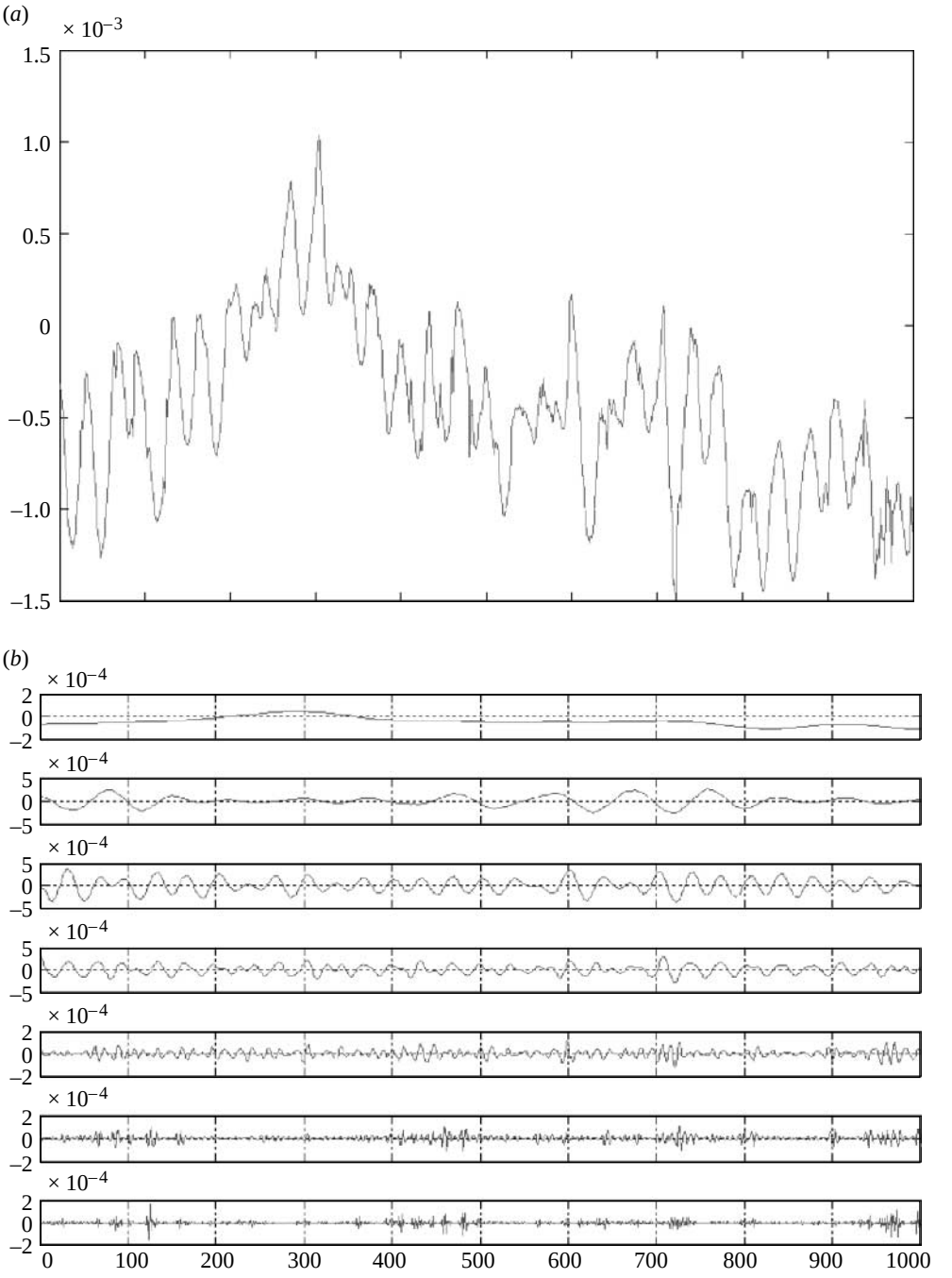

Figure 7. Multi-scale analysis of a milling surface. (*a*) Milled profile; (*b*) multi-scale wavelet representation; (*c*) surface reconstruction (form error, waviness and roughness profiles).

Jiang *et al.* (1997), however, soon identified the phase distortion problems in orthogonal wavelets. Based on biorthogonal wavelets, and using a fast algorithm called 'the lifting scheme' developed at Bell Laboratory by Swelden (1995, 1996),

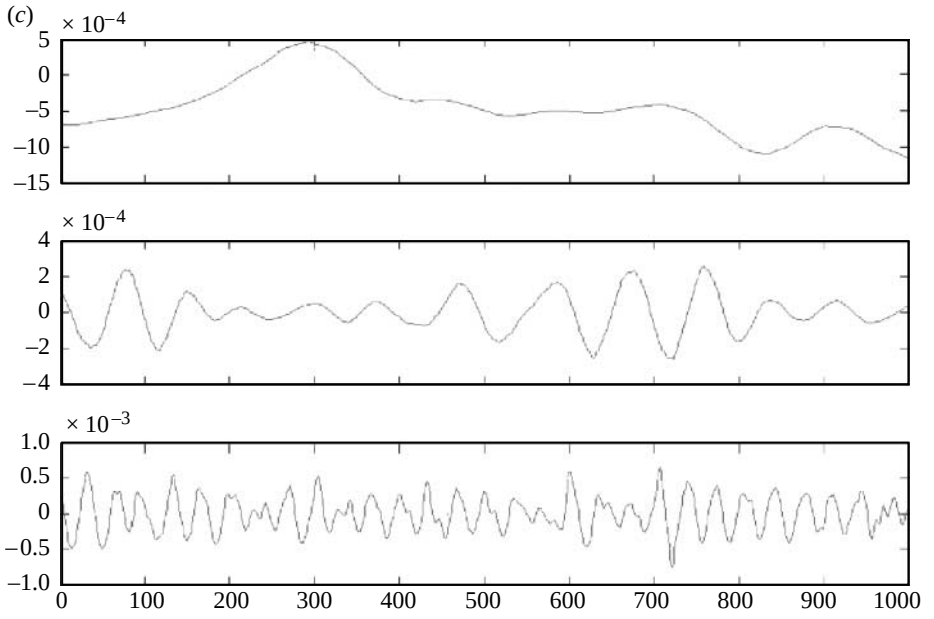

Figure 7. (*Continued.*)

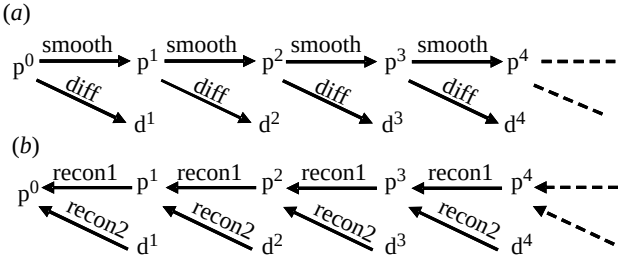

Figure 8. Ladder structures associated with the wavelet transform and wavelet reconstruction. (*a*) Wavelet transformation ladder; (*b*) wavelet reconstruction ladder.

Jiang proposed a new wavelet representation for use with multi-scale surface topography (Jiang *et al.* 2000). This biorthogonal wavelet overcomes the distortion problems that occur with orthogonal wavelets.

Application of the profile biorthogonal wavelet transform consists of constructing a ladder of smooth approximations to the profile (figure 8*a*). The first rung in the ladder is the original profile. Each subsequent rung consists of splitting the profile at that rung into two components, namely a smoother version of the profile, via a smoothing filter, which becomes the next rung, and a component, called the difference profile, which contains information about the difference between the two rungs via a high-pass filter. The action of the smoothing filter and the high-pass filter reduces the number of profile points by half. Each rung in the ladder therefore represents a different scale of the profile.

The smoothing filter and the high-pass filter are designed so that the original profile can be reconstructed perfectly from the final smoothed profile on the last rung and all the difference profiles from the other rungs on the ladder.

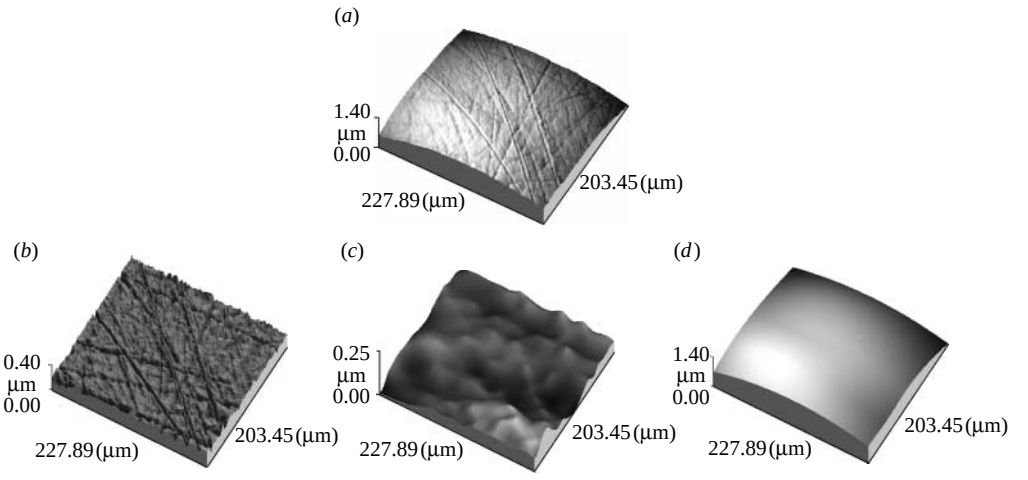

Figure 9. Wavelet decomposition of a precision-lapped ceramic sphere used as a femoral-bearing surface in a replacement hip joint. (*a*) The raw measured surface; (*b*) roughness surface (the short-scale SL surface) S-filter = 0.05 µm, L-filter = 0.10 µm; (*c*) wavy surface (the middle scale SF surface) S-filter = 0.10 µm, F-operator; (*d*) form surface (the long-scale form surface) F-operator.

Reconstruction is achieved by using a second pair of matched reconstruction filters so that at each rung the next lower rung can be reconstructed by adding a filtered version of the smoothed profile with a filtered version of the difference profile from the next rung (figure 8*b*).

A wavelet transform does not consist of a single method (like the Fourier transform), but a multitude of transforms dependent on a 'mother wavelet', which determines the four filters.

This analysis model not only provides a fast algorithm, and in-place calculation, but also has both the 'simplicity' and 'naturalness' for the separation and reconstruction of different multi-scalar components of the surface, with a better metrological transmission characteristic than a Gaussian filter (Jiang *et al.* 2000). The method has now been transferred to ISO/TS 16610-29 for geometrical filtration with adequate theoretical foundation (Jiang 2003) and available software (Taylor Hobson 2006).

A surface biorthogonal wavelet transform has a slightly more complicated ladder structure, but the basic concept is the same. At each rung in the ladder, the surface is split into two components: (i) a smoothed surface component, (ii) a difference surface component that includes three elements, a difference element for the *X* direction and a difference element for the *Y*-direction using the high-pass filter in the respective direction, and a difference element in both *X*- and *Y*-directions with the profile high-pass filter applied in both those directions.

To obtain different scale components of the profile or surface (e.g. roughness, waviness, form, error, etc.), all that is necessary is to set to zero those difference components in the ladder structure that are not part of the scale component, and reconstruct the profile or surface. The reconstructed profile or surface will consist of only the required scales.

Figure 9 shows a decomposition of measurement data representing a precision-lapped ceramic femoral head used in a replacement hip joint. Using only one wavelet decomposition, wavelet filtering of the surface into different passbands,

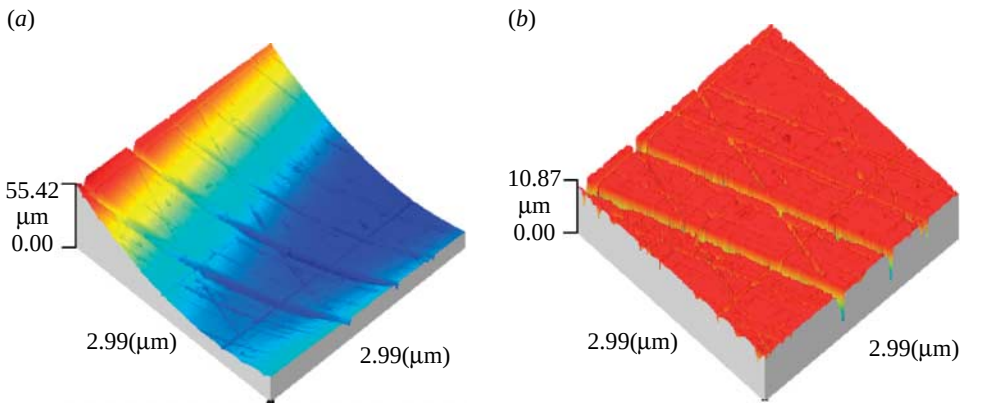

Figure 10. Extraction of honing marks on a plateau-honed surface. (*a*) The raw measured surface; (*b*) the honing marked surface.

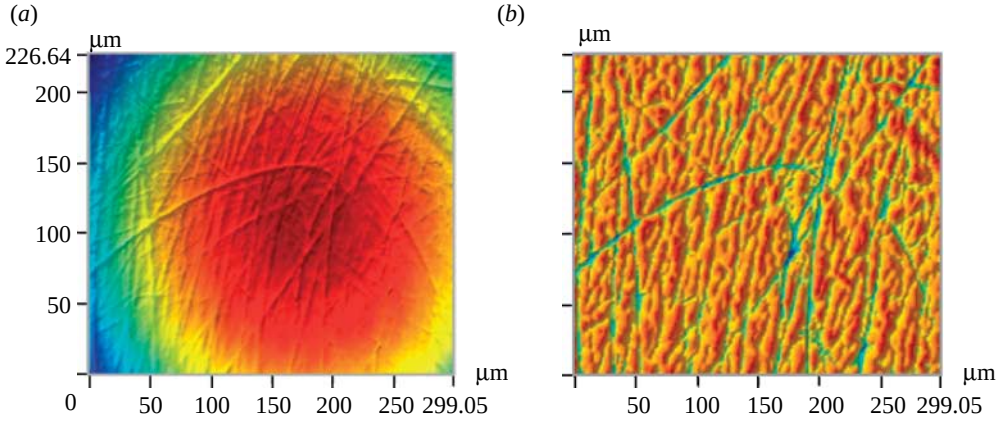

Figure 11. Extraction of wear scores on the surface of a worn ceramic femoral head of an artificial hip joint. (*a*) The raw measured surface; (*b*) the scored worn surface.

equivalent to roughness, waviness and form error components, is easily achieved; consequently, the different passband surfaces can immediately and perfectly be reconstructed within a flexible transmission bank.

The main problem with the biorthogonal wavelet transform is that small shifts in position of the surface can result in a completely different distribution of 'energy' among the wavelet components. In order to extract and reconstruct a surface topography with various scale scratches, such as those in plateau-honed surfaces and worn biomedical surfaces, a complex wavelet model (Jiang & Blunt 2004) was developed according to Kingsbury's dual-tree complex wavelet theory (Kingsbury 1999), to avoid shift-variant problems from affine shifts of the surface. The dual-tree complex wavelet is designed to minimize the shift-variant problem, so that reconstruction of scratches, etc. have considerably less distortion (Jiang & Blunt 2004).

The metrological characteristics of the complex wavelet were examined by Zeng *et al.* (2005), and two industrial examples are shown in figures 10 and 11. More recently, complex ridgelets have been further improved to extract single scratches (Ma *et al.* 2005).

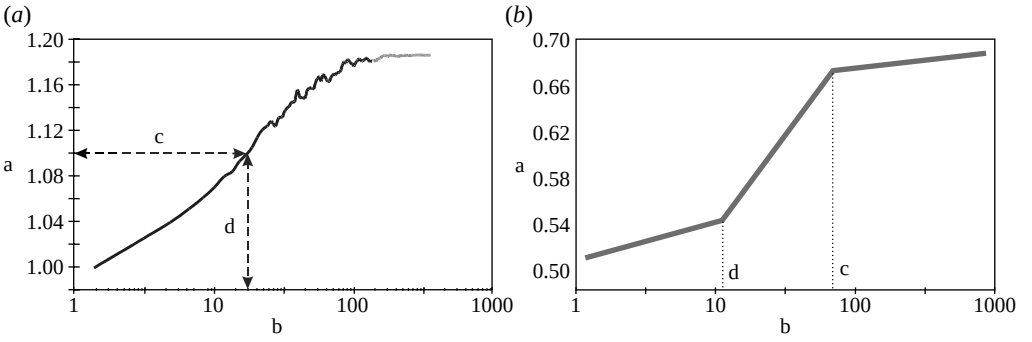

Figure 12. Volume–scale plots. (*a*) Volume–scale plot of a surface. Key: a, volume (μm cubed); b, scale (μm); c, scale; d, volume; (*b*) Idealized volume–scale plot showing. Key: a, volume (μm cubed); b, scale (μm); c, first crossover scale; d, second crossover scale.

(*g*) *Fractal analysis*

In a strict mathematical sense, surfaces are not fractal surfaces, since they do not contain the same type of structures at all scales and become discrete structures at the atomic scale. Surfaces may, however, display fractal-type behaviour over a range of scales. The volume–scale plot (figure 12*a*) is very useful in capturing some complementary behaviour over the observable range of scales. The volume–scale plot is a plot of the log of the volume between an upper and lower envelope of the scale-limited surface of a square horizontal flat as it moves in contact over the upper and lower surface (the upper envelope being the lower locus of the square horizontal flat on the upper surface, the lower envelope being defined analogously) against log-scale of the length of the side of the horizontal square flat. Another type of plot that gives similar information is called area–scale analysis and is based on triangulation rather than the upper and lower envelopes of the surface (Brown & Charles 1993).

Most volume–scale plots of scale-limited surfaces will display several regions where the curve is approximately a straight line. In each of these particular regions, the relationship between the scale s and the volume takes the form of a power law because the volume changes as s^d. The slope of the straight line, on the volume–scale plot, is just the exponent d of the power law.

Over those range of scales where a particular power law is valid (i.e. over the corresponding region of the volume–scale plot where the curve is approximately a straight line), the surface will display self-similarity (that is to say portions of the surface, when enlarged by a suitable amount, will look like the original surface). Hence the surface, over these particular ranges of scales, is approximately a fractal surface with a fractal dimension of $2+d$ (Dubuc *et al.* 1989). Thus, the steeper the slope of the volume–scale plots, the more complicated the surface is for that particular range of scales.

As mentioned above, most volume–scale plots will display several regions where the curve is approximately a straight line. The scale where there is a change in slope from one region approximated by a straight line to another is called a crossover scale. In practice, this change can be ill defined, and so a procedure is necessary for determining the scale at which this change takes place.

The identification of crossover scales is important because they indicate a change in the dominant mechanism affecting the surface of the measurement procedure. For example, figure 12*b* shows a transition from relatively larger scales, where the slope is near zero, to smaller scales, where the slope is steeper. The first crossover scale indicates a change from a relatively smooth surface at larger scales to a rougher surface at smaller scales. Hence, above this first crossover scale, this particular surface can be considered mathematically smooth. The main usage of the crossover points is to identify and characterize the changes in the dominant surface creation process rather than to characterize the functional use of the surface.

3. Current paradigm shift: stochastic surfaces to structured surfaces

All surfaces consist of a collection of features at many different scales that comprise the surface texture. Functional surfaces are 'engineered' to meet functional requirements such as good bearing properties, good electrical contact, formability, paintability and optical properties, as specified by the design intent. The organization of the surface features, the feature types and sizes (together with the material properties, chemistry, etc.) all have a fundamental effect on the resulting function of the surface. The ability to characterize the surface geometry adequately is crucial in the optimization and control of functional surfaces.

In traditional surface creation processes, such as grinding, lapping, polishing, honing, etc., the organization of the surface features is stochastic in nature. Even in turned surfaces that have a fundamental periodic component, there is still a large stochastic element in the surface due to the material shear mechanisms, ploughing and smearing at the tool workpiece interface. Surfaces with a dominant stochastic feature pattern are termed 'stochastic surfaces'; they have been very successfully characterized using techniques based on signal processing (e.g. spectral analysis, autocorrelation functions, material ratio curve, etc.), as discussed in Part I.

Surfaces whose features are organized as a deterministic pattern have recently become economically very important. The deterministic patterns include tessellations (road signs, golf balls), rotationally symmetric patterns (e.g. Fresnel lens) and linear patterns (e.g. diffraction gratings), etc. Even though there may be a small stochastic element within these surfaces, the deterministic pattern dominates. Surfaces with a dominant deterministic feature pattern are here called 'structured surfaces'. All structured surfaces are specifically designed to meet a specific functional requirement. For example, one of the earliest structured surfaces was the modern dimpled golf ball (Taylor 1905) whose functional requirement was to reduce air drag, through better hydrodynamic flow around the ball, so that it could be hit further. A more complete review of structured surfaces can be found in Evans & Bryan (1999).

Surface texture always comprises many features of interest. The defining property of surface texture, which differentiates it from other areas within the GPS system, is that the characteristics are statistical (i.e. mean, maximum, range, etc.), and derived from the individual values of either an attribute of the features (e.g. feature height, area, and volume, etc.) or a relationship between features (e.g. distance between neighbouring features, etc.). In the new areal

surface texture system, the definition of surface texture works for both stochastic surfaces, where the features are the scale-limited portions of the surface, and structured surfaces, where the features are the predetermined surface features.

(a) Segmentation

To identify features on a surface, an automatic method is required to segment the surface into regions of interest. More than 100 years ago, Maxwell (1870) proposed dividing a landscape into regions consisting of hills and regions consisting of dales. A Maxwellian hill is an area from which maximum uphill paths lead to one particular peak, and a Maxwellian dale is an area from which maximum downhill paths lead to one particular pit. By definition, the boundaries between hills are course lines (watercourses), and the boundaries between dales are ridge lines (watershed lines). Maxwell was able to demonstrate that ridge and course lines are maximum uphill and downhill paths emanating from saddle points and terminating at peaks and pits. Recently, the Maxwellian dale (watershed lines) has emerged as the primary tool of mathematical morphology for segmentation of surfaces as preparation for pattern recognition (Scott 2004).

Unfortunately, segmenting a surface into Maxwellian dales can be disappointing since the presence of measurement noise can cause over-segmentation into a large number of insignificant (tiny) shallow dales, rather than relatively few large deep dales, which would result for ideal (noise-free) data. What is required is the merging of insignificant dales into larger significant dales. Scott (2004) has extended Maxwell's definitions, so that a dale consists of a single dominant pit surrounded by a ring of ridge lines connecting peaks and saddle points, and a hill consists of a single dominant peak surrounded by a ring of course lines connecting pits and saddle points. Within a dale or hill, there may be other pits or peaks, but they will all be insignificant compared with the dominant pit or peak.

A mechanism is required to prune the Maxwellian hills and dales to the new extended, definitions, which would reduce the influence of measurement noise, but retain relevant information. Scott (2004) presented a set of necessary and sufficient criteria that all pruning methods must satisfy to ensure that the method is stable and robust. A popular stable and robust pruning method that works well in practice is Wolf pruning (Wolf 1991). In the literature, there are several publicized references to stable and robust pruning methods (Barré & Lopez 2000; Bleau & Leon 2000).

(b) Segmentation applications

The manufacture and fabrication of MEMS and microfluidic devices is now a hugely expanding technology, with applications ranging from electronics to biotechnology. A major hurdle for the mass production and development of these devices is the measurement of the geometry and to a lesser extent, the surface texture. The difficulties lie around the ability to separate and quantify zones of differing planar height and then being able to analyse these zones individually and in relation to each other.

The stable extraction of significant surface features is based on edge detection of significant features and application of segmentation. To separate and quantify zones of differing planar separation, morphological edge detection based on the

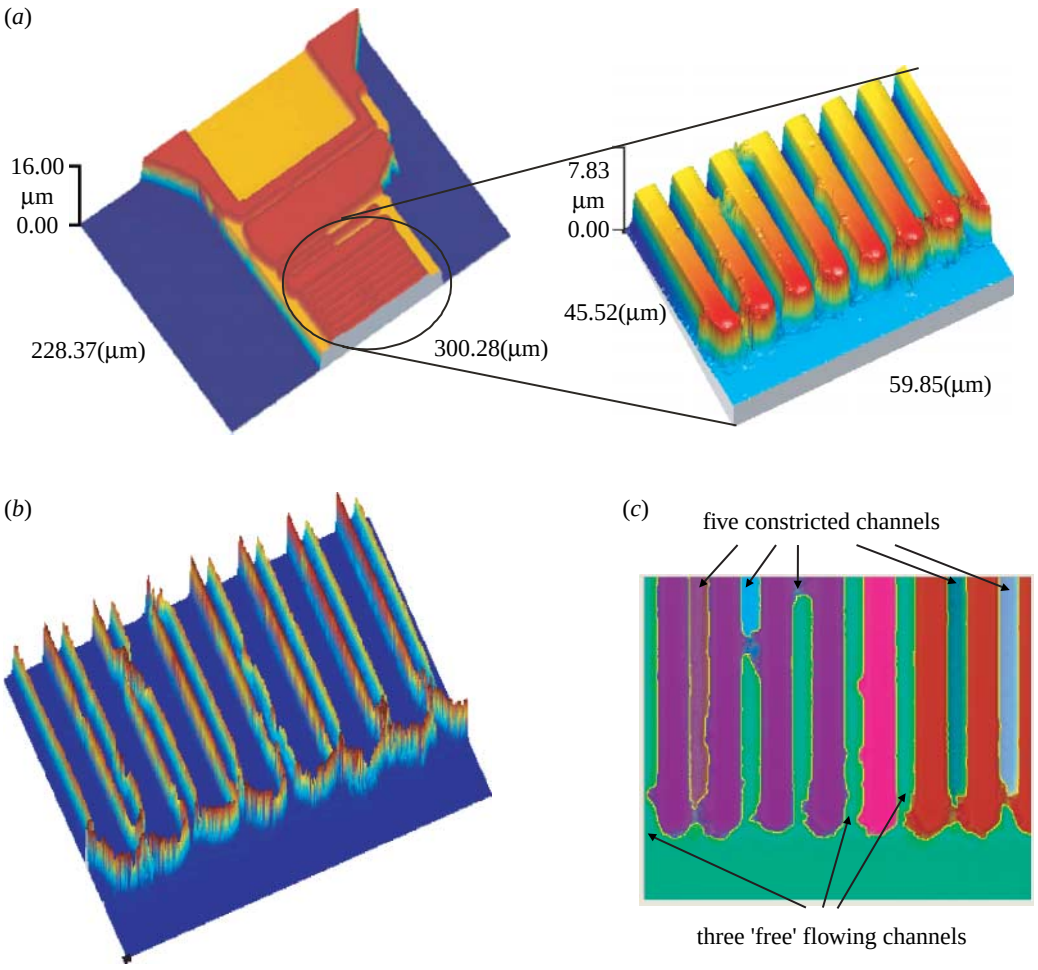

Figure 13. Measurement of a microfluidic plasma device. (*a*) The entrance to the reactor channels are shown in higher magnification; (*b*) Sobel edge image of reactor channels; (*c*) segmented image of device.

Sobel operator is initially applied, and then segmentation with Wolf pruning is used to detect closed contours that bound significant geometrical features. Areas within these closed contours can then be isolated and separately analysed individually or as a feature of the overall geometry. Figure 13 shows an example of the techniques when applied to analysing the planar heights on a microfluidic device. In figure 13*a*, the entrance to the reactor channels is shown at higher magnification. The channels have a close spacing of 3 µm, and the plasma flow and consequent fluid separation is greatly influenced by the channel dimensions and any defect within the channels. Conventional metrology for such devices would involve a visual analysis of each channel individually, which is difficult and time consuming. The result is that many devices are not measured, and are only tested when the complete device is assembled. The result is that scrap rates of as high as 75% are known (Singleton *et al.* 2002).

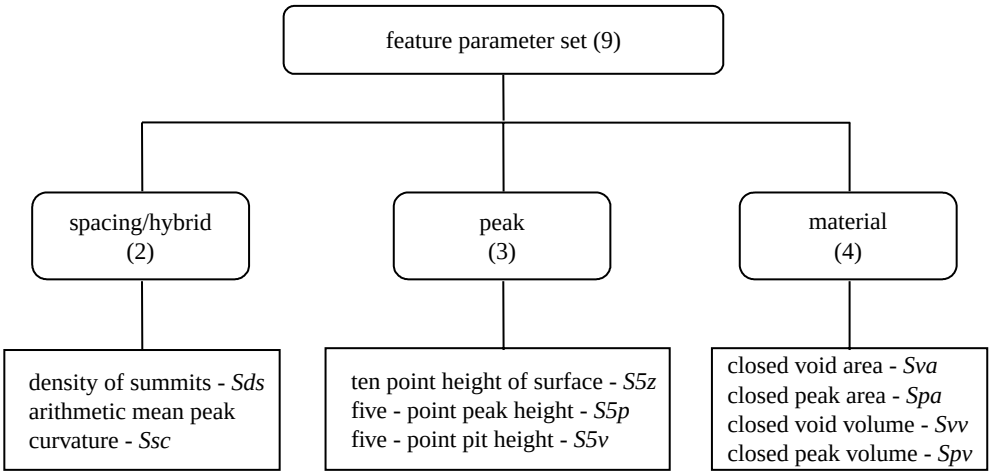

Figure 14. A feature parameter set as given in ISO 25178-2.

By processing the surface data from the device using a Sobel edge operator, the step planes can be distinguished from the base plane, since the edges build a 'fence' to form the close contours. In figure 13*b*, the edges of the step planes form clear boundaries with the base plane, and positions of the step planes can be easily identified. Figure 13*c* displays the result of the segmentation using Wolf pruning and morphological pattern analysis. The whole surface was segmented into nine sections, eight for the channels and one for the base and channel path plane. The edge lines are perfectly consistent with the edge of the channel walls. It is clear that five channels are partially blocked by defects and only three channels could be considered as free-flowing channels.

In conclusion, the segmentation techniques offer the possibility of fast automatic metrology techniques, and these types of techniques can be developed to most features on scale-limited surfaces.

(*c*) *Five steps to a feature parameter*

Feature characterization does not in general have specific feature parameters defined but has instead a toolbox of pattern recognition techniques that can be used to characterize specified features on a scale-limited surface. The feature characterization process consists of five stages: (i) selection of the type of texture feature; (ii) segmentation; (iii) determining significant features; (iv) selection of feature attributes; and (v) quantification of feature attribute statistics. There are nine specifically named feature parameters (figure 14) defined in ISO 25178-2; these parameters are however still defined using the five stages.

(i) *Type of texture feature*

The three main types of texture features are areal features (hills and dales), line features (course and ridge lines) and point features (peaks, pits and saddle points). It is important to select the appropriate type of texture feature for the function of the surface under inspection.

Table 1. Attribute statistics.

attribute statistic	designated symbol	threshold
arithmetic mean of attribute values	mean	—
maximum attribute value	max	—
minimum attribute value	min	—
r.m.s. attribute value	r.m.s.	—
percentage above a specified value	perc	value of threshold in units of attribute
histogram	hist	—
sum of all the attribute values	sum	—

(ii) *Segmentation*

Segmentation is used to determine regions of the scale-limited surface that define the scale-limited features.

(iii) *Determining significant features*

A given 'function' does not interact with all features in the same way; different features interact differently. It is thus essential to determine those features that are functionally significant from those that are not. For each particular surface function, segmentation procedure is required that identifies the significant and insignificant features defined by the segmentation.

(iv) *Selection of feature attributes*

Once the set of significant features has been determined, it is necessary to determine suitable feature attributes for characterization. Most attributes are a measure of size of the feature, e.g. length, area or volume of a feature, or feature density.

(v) *Attribute statistics*

Feature attributes constitute calculation of a suitable statistic for the significant features, a feature parameter, or alternatively a histogram of attribute values. An example of feature attribute statistics is given in table 1.

(*d*) *Structured surfaced with nanoscale features*

There are two basic approaches to the creation of features of specified geometry on the nanosurfaces: 'top-down' and 'bottom-up' approaches. In this paper, surface metrology is associated with the top-down approach, which covers surfaces largely manufactured by ultra-precision machining, micro moulding, embossing and lithographic techniques. Typically, the structures produced are at the micrometre or nanometre scale in one dimension, and tend to be microscale or larger in the other dimensions. As technology advances, the sizes of individual structures are approaching the nanoscale in all three spatial dimensions, which will provide a further challenge to metrologists, especially in terms of instrumentation.

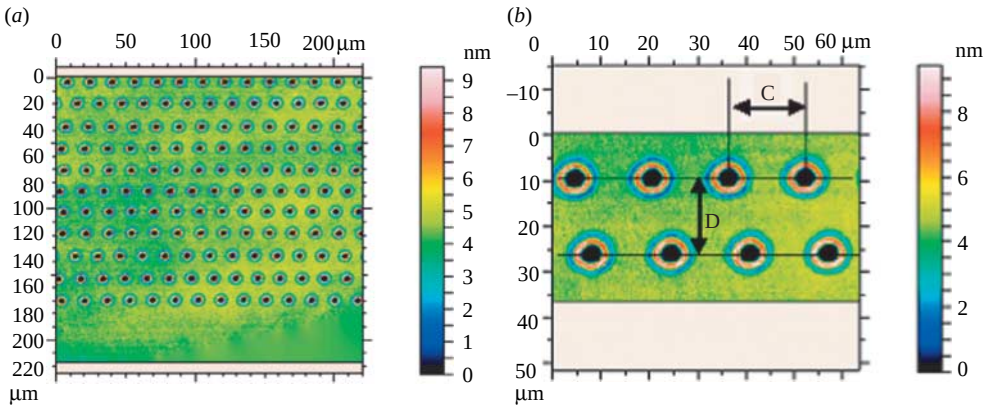

Figure 15. An example for characterization of nanoscale features on structured surface. (*a*) laser zone texturing; (*b*) parameters for laser zone texturing.

(vi) *Feature detection for characterization*

The hard disk drive industry uses a specially structured area on the hard drive to park the hard drive read/write head. This area consists of a series of laser-ablated holes (bumps) that are burned into the disk surface in a structured process referred to as laser zone texturing. The function of the zone is to scrape out air from the air bearing beneath the read/write head and to park the head correctly without damaging the head or disk. An excellent example of structured surface characterization in the quantification of these bumps is shown in figure 15*a*.

The manufacturer calculates a series of parameters for each disk. The first set characterizes the relationship between the bumps and consists of the mean distance between the centres of two adjacent bumps within a row and the mean distance between two adjacent rows of bumps. It can be seen in figure 15*b* that C is the distance between the centre of two adjacent bumps and D is the distance between two adjacent rows of bumps. Segmentation is used to define the extent of each laser-ablated hole, and then the distances are easily calculated.

The second set of parameters characterizes statistics of particular attributes of the bumps and includes the maximum height of the highest bump, the average height of all the bumps, the average diameter of all the bumps, and the difference between the largest and smallest diameters of all the bumps. The diameter is calculated as the least squares circle that best fits the segmentation boundary of the bump. The above analysis needs to be carried out automatically and in less than 2 s.

In conclusion, the segmentation technique with feature analysis offers the possibility of fast automatic metrology procedures. Moreover, such procedures can be developed for most features on nanoscale surfaces.

4. Current paradigm shift: simple geometries to complex freeform geometries

(*a*) *Introduction*

In many technologically advanced industries, such as optics, the shape of the surfaces of manufactured objects is becoming much more complicated than simple

geometrical shapes. Unlike conventional surfaces, these advanced surfaces have no axes of rotation and in the future could have almost any designed shape. These latter geometrical surface shapes are called freeform surfaces (Clayor *et al.* 2004).

The geometry of freeform surfaces cannot be described by a single universal equation, as is the case for aspheric surfaces, but a myriad of equations including toroidal, biconic, microstructures (such as V-groove, lenticulation and echells, pyramid), NURBS, etc. Clayor proposed that micro-lens arrays also belong to freeform since they have the same aspects in fabrication, alignment and measurement (Clayor *et al.* 2004; Jiang *et al.* 2007).

Over the past decade, the design and manufacture of advanced optics has begun to include freeform optical elements and micro-structured optical surfaces, which are critical components in high added-value products such as mobile phone cameras, laser printers, flat-bed scanners, displays, telecommunications, photonics (broadband optical fibre connectors) and biomedical devices. Freeform surfaces allow these optical components to contain less 'glass', making them lighter, cheaper to manufacture, and in most cases perform better (ASPE 2004; Lee 2005). The rapidly increasing use of ultra-precision freeform surfaces is, however, not limited to the optics field: bio-implants such as knee prostheses use freeform surfaces as the bearing components. One of the primary advances in this field is freeform hard-bearing couples, requiring micrometre scale form control with nanometric surface topography control (Blunt & Charlton 2005; Bills *et al.* 2006). The next generation of overwhelmingly large telescopes will require complex freeform segment mirrors of dimension 1–2 m with better than 20 nm form accuracy and 5 nm surface finish (Shore & Burman 2004).

Ultra-precision multi-axis freeform machining, single point diamond turning, Computer Numerical Control (CNC) milling, CNC grinding and CNC polishing (ASPE 2004; Optonet Workshop 2004; Hong Kong 2005) constitute an enabling technology that allows the designed freeform surface to be fabricated. However, a fundamental difficulty, relating to the ever-expanding introduction of freeform surfaces, is how to measure and characterize such surfaces with the required sub-micrometre form accuracy and sub-nanometre surface texture.

(*b*) *Freeform surface metrology*

At present, due to the geometrical complexities of freeform surfaces, the achievement of a superior freeform surface still depends largely on the experience and skills of machine operators through an expensive trial-and-error approach. However, the measurement and characterization techniques for freeform surfaces are under development.

(i) *Classification of freeform surfaces*

Freeform surfaces have been classified into three kinds according to their applications as follows (Jiang *et al.* 2007).

Class 1: Surfaces that include steps, edges and facets. An example is the Fresnel lens that is used to collimate the light in a lighthouse and in some modern car headlights.

Class 2: Surfaces that have a tessellated pattern, i.e. a repeated structure over the surface. An example is a 3M trizac abrasive surface, which consists of an array of triangular-based micrometre-sized pyramids.

Class 3: Smooth surfaces, i.e. surfaces designed with no steps, edges or patterns, but relying purely on the global geometry. An example is the overwhelmingly large telescope project (Shore & Burman 2004), which requires complex freeform segment telescope mirrors.

(ii) *Measurement techniques of freeform surfaces*

There is currently no mature traceable measurement methodology for the complete range of complex geometric surfaces. Some traditional measurement techniques ranging from contact to non-contact and from points to areal measurement are partially used for freeform surface measurement. For example:

(i) SEM/AFM have been used for measuring the surface topography of single features of microlenses (Takeuchi *et al.* 2004; Lee *et al.* 2006; Orhan *et al.* 2006).
(ii) Contact profilometry with large measurement range such as the Talysurf PGI has been used to measure the optical lenses (Taylor Hobson 2006).
(iii) Phase shifting interferometry (PSI) may be the most widely used method for super smooth surface such as the wafer surface. White light interferometry has been widely used for the measurement of surfaces with steps, edges and facets.
(iv) Mach–Zehnder/Twyman–Green interferometer with a null lens has been used for the measurement of aspheric lenses (Reichelt *et al.* 2005). One method for aspheric metrology without null lenses is sub-aperture interferometry. The whole surface of the part can be measured by combining or 'stitching' the sub-aperture measurements.
(v) Computer-generated holography has been widely used to test rotationally symmetric surfaces for many years. A computer-generated holograph (CGH) can be thought of as a binary representation of the interferogram, or hologram, that would be recorded if the aspheric wavefront coming from a perfect aspheric surface interferes with the reference beam. The CGH and the interference fringes produced by the interference of the reference wavefront and the wavefront produced by the mirror under test are used to generate a moiré pattern. This pattern gives the difference between the CGH and the interference. Current systems can achieve 1/50 wavelength accuracy from a hologram diameter of 50 mm (Brinkmann *et al.* 1998; Burge & Wyant 2004).
(vi) Geometry measuring machine (GEMM) is an areal shape-measuring instrument. It uses a Twyman–Green phase measuring interferometer as a curvature sensor. GEMM can measure a maximum of 110 mm diameter, with a 4 m radius of curvature (Chang *et al.* 2004; Machkour-Deshayes *et al.* 2006).
(vii) Swing arm profilometer produces a two-dimensional profile of an aspheric surface. A small interferometer or a stylus serves as a sensor mounted on the swing arm to measure the form deviation (King *et al.* 2006). Current swing-arm profilometers are intended as proof-of-concept devices and have the

capability to measure concave surfaces up to 1 m in diameter with a minimum radius of curvature of 1.75 m. Another method is to measure the local curvature of the surface along the direction of the profile, and then reconstruct the profile from the curvature measurements (Elstner *et al.* 2001; Schulz 2001).

The measurement of freeform surface topography on ultra precision and nanoscale still leaves a significant technological deficit, where available measurement systems have problems in achieving the large dynamic range with sufficient resolution. There are urgent requirements for innovation and new measurement instruments.

(iii) *Characterization of freeform surface*

Beyond the inherent technical challenges in freeform surface measurement, freeform surface characterization is another obstacle to freeform surface manufacture. Being different from a simple geometry surface fit (Forbes 1990, 2005; Stout *et al.* 1993; McBride & Cross 1996; Taylor Hobson 2006), the form accuracy of a freeform surface depends on the fitting accuracy of the measured surface and a reference template (a complex nominal surface). Currently, there is a lack of uniform terminology and absence of consistent mathematical fitting techniques.

A new fitting methodology has been proposed (Jiang *et al.* 2007), which is designed for smooth freeform surfaces, and assumes that the measured surface is a portion of the nominal surface. In order to reach a high fitting accuracy of one part in 10^7, a two-stage fitting method has been investigated, in which an initial fitting procedure is performed to supply a rough position and a final fitting procedure to improve the accuracy.

A structured region signature technique has been developed for the initial rough fitting (Zhang *et al.* in press). In this method, a suitable sphere is used with its centre located on the measured surface. Those measured points that lie close to the boundary of the sphere with the measured surface (figure 16*a*) form an approximate circle. These points are projected onto a best-fit plane generated from all the measurement points within this sphere (figure 16*b*).

The signed projection distance d of each of the boundary points, and the polar angle θ form a signature profile (figure 16*c*) for the point on the measured surface at the centre of the sphere. Signatures are calculated at locations uniformly sampled on the reference template. The template location yielding a signature closest to that of the measurement surface is taken as the best approximation to the rough position.

Final fitting is employed to reach higher accuracies. If the reference template is a point cloud, an iterative closed point method (Besl & McKay 1992) can be adopted. Otherwise, a Levenberg–Marquardt technique (Fitzgibbon 2003) can be applied to a smooth continuous template function reconstructed from the cloud of points using standard functions, e.g. radial basis functions, NURBS, etc.

A computing simulation is given below. A small portion of dimension $40\times40\,\mathrm{mm}^2$, as shown in figure 17*a*, is extracted from a freeform surface. It is transformed to an arbitrary position as the initial location of the measurement surface (figure 17*b*), and Gaussian noise N(0, 0.2 μm) is added to represent measurement error. Using the structured region signature method, a rough

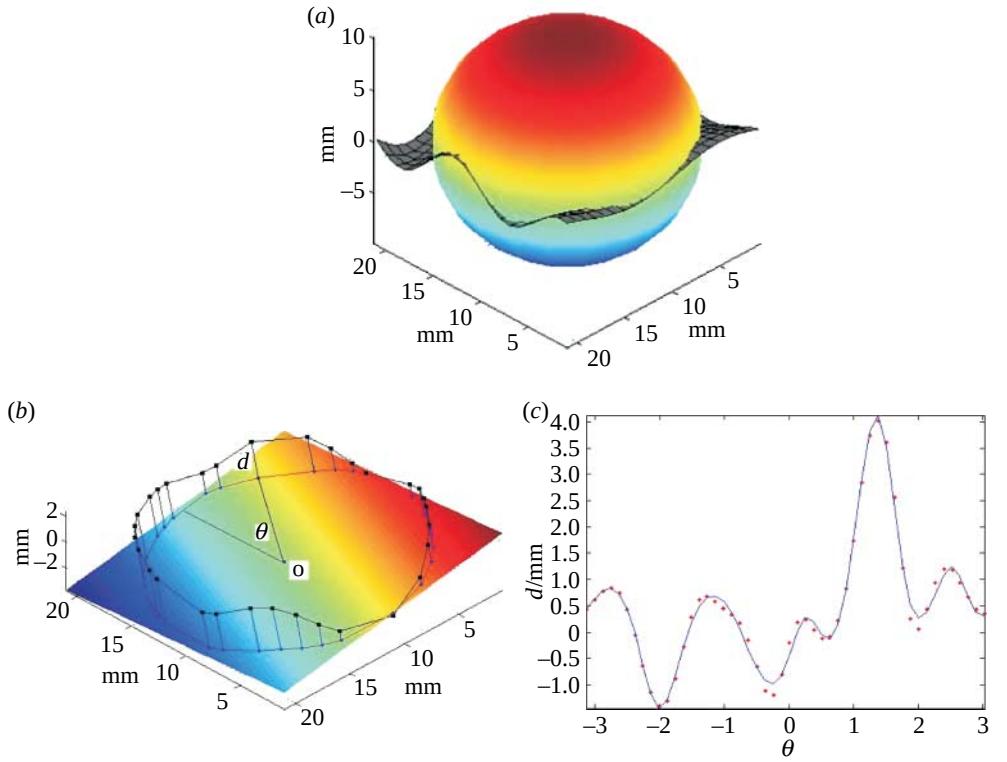

Figure 16. Definition of structured region signature. (*a*) Inscribed sphere; (*b*) projecting to the best-fitted plane; (*c*) signature profile.

fitting position is obtained (figure 17*c*). Final fitting is performed to optimize the fitting result as shown in figure 17*d*. The rotation and translation errors in this case are of the order of 10^{-4} degree and 10^{-5} μm, respectively (Zhang *et al.* accepted).

5. Conclusions

Throughout parts I and II of this paper, the development of the discipline of surface metrology has been tracked according to its paradigm shifts in order to meet new requirements demanded by multi-dimensional technology and consequent engineering evolutions.

The genesis of the surface metrology discipline started centuries ago, with the investigations of da Vinci, Amonton and Coulomb into the friction between surfaces of a moving body. Through the first investigation into profilometers, Abbott made practical and theoretical contributions during the 1930s, together with the 'Material Ratio Curve', which is still used today. Signal processing theory led to a digital paradigm shift. Finally, there was the development of wide vertical-range instruments. These three developments build a complete philosophical model for changes up to the 1990s.

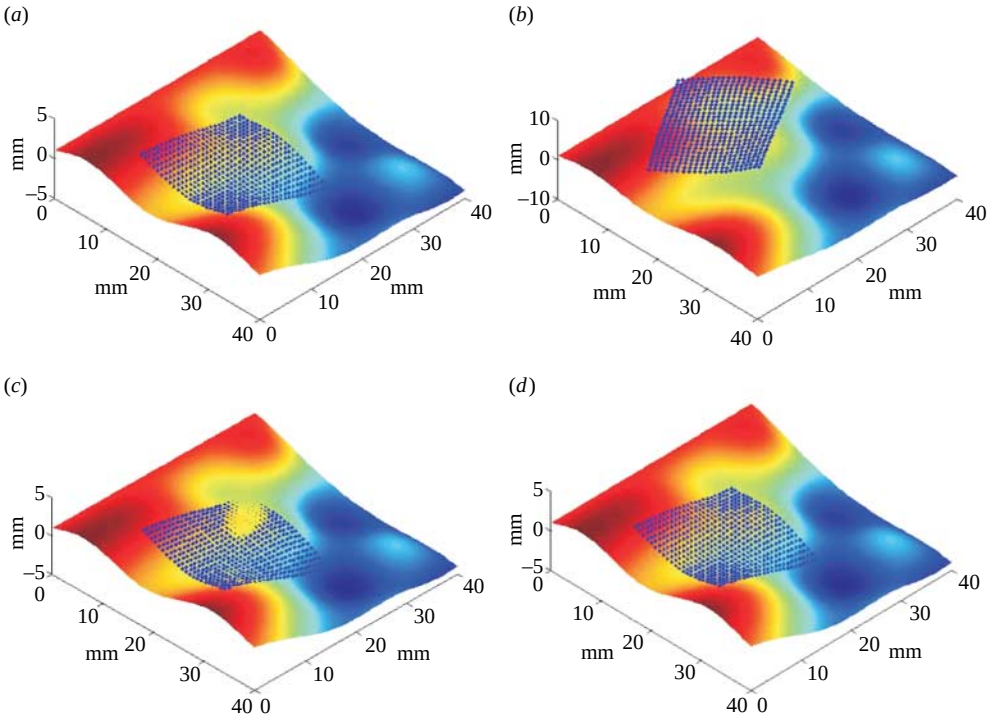

Figure 17. An example of the two-stage fitting. (*a*) An ideal position; (*b*) transforming to a new position; (*c*) initial fitting result; (*d*) final fitting result.

Following these historical developments, this paper describes a disciplined development of the philosophies in the current paradigm shift. These techniques include measurement, instrumentation, filtration, characterization and standardization. This paper considers new applications for this constantly evolving discipline.

The paper indicates that metrology for structured surfaces and freeform surfaces will be the big challenge for surface metrology. This statement is made because the scale of surface texture is beginning to approach some of the geometrical features in MEMS/NEMS devices and microlenses. Moreover, form deviations and surface finish for telescope mirrors, for example, are approaching one part in 10^8.

Although in both parts of this review paper a number of issues have been discussed, they are by no means a comprehensive list, but are sufficient to indicate the nature and scope of the development of the discipline of surface metrology. One subject that has not been covered concerns surface systems as opposed to single surfaces. Although the concern of this paper has been single surface properties, consideration of the contact between and the relative movement of *surfaces* is also of the greatest importance.

X.J. gratefully acknowledges the Royal Society under a Wolfson-Royal Society Research Merit Award. The authors gratefully acknowledge the Research Committee of the University of Huddersfield for supporting funds for this work and the directors of Taylor Hobson Limited for permission to publish.

References

ASPE, 2004 *Winter topical meeting*: *Free-form optics: design, fabrication, metrology, assembly. 4–5 February North Carolina, USA*.

Barré, F. & Lopez, J. 2000 Watershed lines and catchment basins: a new 3D-motif method. *Int. J. Mech. Tool Manufact.* **40**, 1171–1184. (doi:10.1016/S0890-6955(99)00118-2)

BCR. Contract No 3374/1/0/170/90/2 1990 *An integrated approach to 3D surface measurement*, University of Birmingham and L'Ecole Centrale de Lyon.

Besl, P. J. & McKay, N. D. 1992 A method for registration of 3-D shapes. *Trans. Pattern Anal. Mach. Intell.* **14**, 239–256. (doi:10.1109/34.121791)

Bills, P., Blunt, L. & Jiang, X. 2006 A metrology solution for determination of form deviation and wear—in orthopaedic joint replacements. In *33rd Leeds–Lyon Symposium on Tribology*, 12–15 September, 2006, Leeds, UK.

Bleau, A. & Leon, L. J. 2000 Watershed-based segmentation and region merging. *Comput. Vis. Image Und.* **77**, 317–370. (doi:10.1006/cviu.1999.0822)

Blunt, L. & Charlton, P. 2005 The application of optics polishing to free form knee implants. In *Proc. of EUSPEN 2006, Baden, Austria, 27th–June 1st May.*

Blunt, L. & Jiang, X. 2003 *Advanced techniques for assessment surface topography—development of a basis for the 3D surface texture standards "SURFSTAND"*, Kogan Page Science.

Blunt, L., Jiang, X. & Stout, K. J. 1999 Developments in 3D surface metrology, laser metrology and machine performance IV, Lamdamap'99, 255–266.

Brinkmann, S., Schreiner, R., Dresel, T. & Schwider, J. 1998 Interferometric testing of plane and cylindrical workpieces with computer-generated holograms. *Opt. Eng.* **37**, 2506–2511. (doi:10.1117/1.601759)

Brown, C. A. & Charles, P. D. 1993 Fractal analysis of topographic data by the patchwork method. *Wear* **161**, 61–67. (doi:10.1016/0043-1648(93)90453-S)

Burge, J. H. & Wyant, J. C. 2004 Use of computer generated holograms for testing aspheric optics. In *Proc. of ASPE winter topical meeting: free-form optics: design, fabrication, metrology, assembly, 4–5 February North Carolina, USA*.

Chang, K. B., Saiag, T., Wang, Q., Soons, J., Polvani, R. S. & Griesmann, U. 2004 The geometry measuring machine (GEMM) project at NIST, ASPE2004 winter topical meeting. In *Pro. of ASPE Winter topical meeting: free-form optics: design, fabrication, metrology, assembly. 4–5 February North Carolina, USA*.

Chen, X., Raja, J. & Simanapalli, S. 1995 Multi-scale analysis of engineering surfaces. *Int. J. Mach. Tools Manufact.* **35**, 231–238. (doi:10.1016/0890-6955(94)P2377-R)

Chui, C. K. 1992 *An introduction on wavelets*. Philadelphia, PA: SIAM.

Clayor, N. E., Combs, D. M., Lechuga, O. M., Mader, J. J. & Udayasankaran, J. 2004 An overview of freeform optics production. In *Proc. of ASPE Winter topical meeting: free-form optics: design, fabrication, metrology, assembly, 4–5 February, North Carolina, USA*.

Daubechies, I. 1992 *Ten lectures on wavelets*, 1st edn. Philadelphia, PA: SIAM.

De Chiffre, L. & Nielsen, H. S. 1987 A digital system surface roughness analysis of plane and cylindrical parts. *Precision Eng.* **9**, 59–64. (doi:10.1016/0141-6359(87)90054-7)

DIN 4776: 1990 Kenngrößen Rk, Rpk, Rvk, Mr1, Mr2 zur Beschreibug des Materialanteils im Rauheitsprofil—Meßbedingungen und Auswerteverfahren, Deutsche Norm, Berlin: Beuth Verlag GmbH.

Dong, W. P., Sullivan, P. J. & Stout, K. J. 1994*a* Comprehensive study of parameters for characterizing three-dimensional surface topography III: parameters for characterizing amplitude and some functional properties. *Wear* **178**, 29–43. (doi:10.1016/0043-1648(94)90127-9)

Dong, W. P., Sullivan, P. J. & Stout, K. J. 1994*b* Comprehensive study of parameters for characterizing three-dimensional surface topography IV: parameters for characterizing spatial and hybrid properties. *Wear* **178**, 45–60. (doi:10.1016/0043-1648(94)90128-7)

Dubuc, B., Zucker, S. W., Tricot, C., Quiniou, J. F. & Wehbi, D. 1989 Evaluating the fractal dimension of surfaces. *Proc. R. Soc. A* **425**, 113–127. (doi:10.1098/rspa.1989.0101)

E.C. Contract No SMT4-CT98-22561 1998 The development of a basis for three-dimensional surface roughness standards.

Elstner, C., Gerhardt, J., Thomsen-Schmidt, P., Schulz, M. & Weingartner, I. 2001 Reconstruction surface profiles from curvature measurements. *Optik* **113**, 154–158.

Evans, C. J. & Bryan, James B. 1999 'Structured', 'textured' or 'engineered' surfaces. *Ann. CIRP* **48/2**, 541–556.

Fitzgibbon, A. W. 2003 Robust registration of 2D and 3D point sets. *Image Vision Comput.* **21**, 1145–1153. (doi:10.1016/j.imavis.2003.09.004)

Forbes, A. B. 1990 Least squares best fit geometry elements. In *Algorithms for approximation* (eds J. C. Mason & M. G. Cox), pp. 311–319. London, UK: Chapman and Hall.

Forbes, A. B. 2005 Algorithms for structured Gauss-Markov regression. In *Algorithms for approximation V* (eds A. Iske & J. Levesley), pp. 167–185. London, UK: National Physical Laboratory.

Greenwood, J. A. & Williamson, J. B. P. 1966 Contact of nominally flat surface. *Proc. R. Soc. A* **295**, 300–319. (doi:10.1098/rspa.1966.0242)

Grieve, D. J., Kaliszer, H. & Rowe, G. W. 1970 A 'normal wear' process examined by measurements of surface topography. *Ann. CIRP* **18/4**, 585–592.

Hong Kong, 2005 Workshop on: advances in design and fabrication of freeform optics, Hong Kong, 21st–23rd March.

ISO 4287: 1997 Geometrical product specifications (GPS)—surface texture: profile method—terms, definitions and surface texture parameters.

ISO/TS 17450-2: 2002 Geometrical product specifications (GPS)—General concepts—part 2: basic tenets, specifications, operators and uncertainties.

ISO 1101: 2004 Geometrical product specifications (GPS) Geometrical tolerancing, tolerances of form, orientation, location and run-out.

ISO/TS CD 25178-2: 2006 Geometrical product specification (GPS)—surface texture: areal—part 2: terms, definitions and surface texture parameters.

ISO/TS CD 25178-3: 2006 Geometrical product specification (GPS)—surface texture: areal—part 3: specification operators.

Jiang, X. 2003 Chapter 5: multi-scalar filtration methodology. In *Advanced techniques for assessment surface topography—development of a basis for the 3D surface texture standards*, (eds L. Blunt & X. Jiang), Kogan Page Science.

Jiang, X. 2006 *Standardisation in surface metrology*, the Scientific Technical Committee "S" (Surface) meeting, International Academy of Production Engineering, 24 August 2006, 55th General Assembly, Kobe, Japan.

Jiang, X. & Blunt, L. 2003 Surface analysis techniques to optimise the performance of CNC machine tools, *Laser metrology and machine performance V, Lamdamap'2003*, 17th July, University of Huddersfield, UK.

Jiang, X. & Blunt, L. 2004 Third generation wavelet for the extraction of morphological features from micro and nano scalar surfaces. *Wear* **257**, 1235–1240. (doi:10.1016/j.wear.2004.06.006)

Jiang, X. & Li, Z. 1994 The development Wavelet spectral analysis system for surface characterization, NSFC No: 59375255, China.

Jiang, X., Blunt, L. & Stout, K. J. 1997 *Recent development in the characterization technique for bioengineering surfaces*. In *Transactions of 7th Int. Conf. metrology and properties of engineering surface, 2nd–4th April 1997*.

Jiang, X., Blunt, L. & Stout, K. J. 2000 Development of a lifting wavelet representation for characterization of surface topography. *Proc. R. Soc. A* **456**, 1–31. (doi:10.1098/rspa.2000.0506)

Jiang, X., Scott, P. & Whitehouse, D. J. 2007 Freeform surface characterization—a fresh strategy. *Ann. CIRP* **56/1**, 553–556.

King, C. W., Callender, M. J., Efstathiou, A., Walker, D. D., Gee, A. E., Lewis, A. J., Oldfield, S. & Steel, R. M. 2006 A 1 m swing-arm profilometer for large telescope mirror element. In *Proc. of ASPE 2006*.

Kingsbury, N. 1999 Image processing with complex wavelets. *Phil. Tran. R. Soc. A* **357**, 2543–2560. (doi:10.1098/rsta.1999.0447)

PROCEEDINGS OF THE ROYAL SOCIETY A MATHEMATICAL, PHYSICAL & ENGINEERING SCIENCES

Lee, W. 2005 Market trends and applications of ultra-precision freeform machining technology, *Workshop on Advances in design and fabrication of freeform optics, Hong Kong*, 21st–23rd March.

Lee, C. L., Choi, H. W., Gu, E., Dawson, M. D. & Murphy, H. 2006 Fabrication and characterization of diamond micro-optics. *Diam. Relat. Mater.* **15**, 725–728. (doi:10.1016/j.diamond.2005.09.033)

Lonardo, P. M., Trumpold, H. & DeChiffre, L. 1996 Progress in 3D surface microtopography characterization. *Ann. CIRP* **45/2**, 589–598.

Ma, J., Jiang, X. & Scott, P. 2005 Complex ridgelets for shift invariant characterization of surface topography with line singularities. *Phys. Lett. A* **344**, 423–431. (doi:10.1016/j.physleta.2005.06.091)

Machkour-Deshayes, N., Stoup, J., Lu, J., Soons, J., Griesmann, U. & Polvani, R. S. 2006 Form profiling of optics using the geometry measuring machine and the M-48 CMM at NIST. *J. Res. Natl Inst. Stand. Technol.* **111**, 373–384.

Maxwell, J. C. 1870 On hills and dales. *The London, Edinburgh, and Dublin Phil. Mag. and J. Sci.* Series 4, **40**, 421–427.

McBride, J. W. & Cross, K. J. 1996 The measurement and analysis of the three-dimensional form of curved surfaces. *Int. J. Mach. Tools Manufact.* **36**, 597–610. (doi:10.1016/0890-6955(95)00051-8)

Nayak, P. R. 1971 Random process model of rough surface. *Tran. ASME, J. Lubric. Technol.* **39**, 398–407.

Optonet Workshop 2004 *Ultra Precision Manufacturing of Freeform Optics and Microstructures, Jena, 4th–5th, May 2004*.

Orhan, J.-B., Parashar, V. K., Sayah, A. & Gijs, M. A. M. 2006 Fabrication of three-dimensional microlens arrays in sol-gel glass. *Microelectron. Eng.* **83**, 1329–1332. (doi:10.1016/j.mee.2006.01.045)

Peters, J. *et al.* 2001 Contribution of CIRP to the development of metrology and surface quality evaluation during the last fifty years. *Ann. CIRP* **50/2**, 471–488.

Reichelt, S., Bieber, A., Aatz, B. & Zaoppe, H. 2005 Micro-optics metrology using advanced interferometry. *Proc. SPIE* **5856**, 437–446. (doi:full_text)

Research Council, UK 2004 True to form. *Basic technology*. See http://www.rcuk.ac.uk/basictech/projects.htm.

Royal Society and Royal Academy of Engineering Report 2004, *Nanoscience and nanotechnologies: opportunities and uncertainties*. See www.royalsoc.ac.uk.

Sayles, R. S. & Thomas, T. R. 1977 Measurement of the statistical microgeometry of Engineering surfaces. In *Proc. 1st Joint Polytechnic Symp. manufacturing engineering, Leicester. Leicester Polytechnic*.

Schulz, M. 2001 Topography measurement by a reliable large-area curvature sensor. *Optik* **112**, 86–90.

Scott, P. J. 2004 Pattern analysis and metrology: the extraction of stable features from observable measurements. *Proc. R. Soc. A* **460**, 2845–2864. (doi:10.1098/rspa.2004.1291)

Shore, P. & Burman, P. 2004 Manufacture of large mirrors for ELTs: a fresh perspective, optical fabrication, testing, and metrology. *Proc. SPIE* **5252**, 55–62. (doi:10.1117/12.514698)

Singleton, L., Leach, R., Lewis, A., & Cui, Z. 2002 *Report on the analysis of the MEMSTAND survey on standardisation of microsystems technology*. MEMSTAND Project IST-2001-37682.

Stedman, M. 1987 Basis for comparing the performance of surface-measuring machines. *Prec. Eng.* **9**, 149–152. (doi:10.1016/0141-6359(87)90032-8)

Stout, K.J., Sullivan, P.J., Dong, W.P., Mainsah, E., Luo, N., Mathia, T. & Zahyouani H. 1993 *The development of methods for the characterization of roughness in three dimensions*, 1st edn. Commission of the European Communities.

Swelden, W. 1995 *The lifting scheme: a custom-design construction of biorthogonal wavelets*. Murry Hill, NJ: Bell Laboratories.

Swelden, W. 1996 *The lifting scheme: a construction of second generation wavelets*. Murry Hill, NJ: Bell Laboratories.

PROCEEDINGS OF THE ROYAL SOCIETY A MATHEMATICAL, PHYSICAL & ENGINEERING SCIENCES

Takeuchi, H., Yosizumi, K. & Tsutsumi, H. 2004 Ultrahigh accurate 3-D profilometer using atomic force probe of measuring nanometer, *Winter topical meeting: free-form optics: design, fabrication, metrology, assembly. 4–5 February, North Carolina, USA*.

Taylor, W. 1905 An improvement in golf balls, British Patent No 18 688, British Patent Office, London UK.

Taylor Hobson Ltd. 2006 Form Talysurf PGI Aspheric Measurement Systems. See http://www.taylor-hobson.com/optics_ftspgi.htm.

Teague, E. C., Scire, F. E., Baker, S. M. & Jensen, S. W. 1982 Three-dimensional stylus profilometry. *Wear* **83**, 1–12. (doi:10.1016/0043-1648(82)90335-0)

Thomas, T. R. 1998 Trends in surface roughness. *Int. J. Mach. Tools Manufact.* **38**, 405–411. (doi:10.1016/S0890-6955(97)00084-9)

Vorburger, T. V., Dagata, J. A., Wilkening, G. & Iizuka, K. 1998 Characterization of surface topography. In *Beam effects, surface topography and depth profiling in surface analysis* (eds A. W. Czanderna, T. E. Madey & C. J. Powell). New York, NY: Plenum Press.

Whitehouse, D. J. 1994 *Handbook of surface metrology*. Bristol, UK; Philadelphia, PA: Inst. of Physics.

Whitehouse, D. J. & Phillips, M. J. 1982 Two dimensional discrete properties of random surfaces. *Phil. Trans. R. Soc. A* **305**, 441–468. (doi:10.1098/rsta.1982.0043)

Williamson, J. P. B. 1967–1968 Microtopography of surfaces. In *Proc. Inst. Mech. Eng.* 182 Pt.3K, 21–30.

Wolf, G. W. 1991 A Fortran subroutine for cartographic generalization. *Comput. Geosci.* **17**, 1359–1381. (doi:10.1016/0098-3004(91)90002-U)

Zeng, W., Jiang, X. & Scott, P. 2005 Metrological characteristics of dual tree complex wavelet transform for surface analysis. *Meas. Sci. Technol.* **16**, 1410–1417. (doi:10.1088/0957-0233/16/7/002)

Zhang, X., Jiang, X., & Scott, P. In press. Free-form surface fitting method for precision metrology. In *Proc. 11th Int. Conf. Metrology and Properties of Engineering Surface*, Huddersfield, UK, 17–20 July 2007.